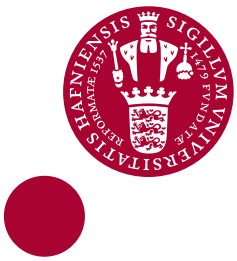

Neutrino oscillation studies with IceCube-DeepCore

Aartsen, M.G.; Abraham, K.; Ackermann, M.; Adams, J.; Aguilar, J.A.; Ahlers, M.; Ahrens, M.; Altmann, D.; Anderson, T.; Ansseau, I.; Koskinen, David Jason; Medici, Morten Ankersen; Larson, Michael James; Sarkar, Subir; Wolf, Michael Marc

Published in:
Nuclear Physics B

DOI:
10.1016/j.nuclphysb.2016.03.028

Publication date:
2016

Document version
Publisher's PDF, also known as Version of record

Available online at www.sciencedirect.com

ScienceDirect

Nuclear Physics B 908 (2016) 161–177

NUCLEAR PHYSICS B

www.elsevier.com/locate/nuclphysb

Neutrino oscillation studies with IceCube-DeepCore

M.G. Aartsen [b], K. Abraham [ag], M. Ackermann [aw], J. Adams [p], J.A. Aguilar [l], M. Ahlers [ad], M. Ahrens [an], D. Altmann [x], T. Anderson [at], I. Ansseau [l], M. Archinger [ae], C. Arguelles [ad], T.C. Arlen [at], J. Auffenberg [a], X. Bai [al], S.W. Barwick [aa], V. Baum [ae], R. Bay [g], J.J. Beatty [r,s], J. Becker Tjus [j], K.-H. Becker [av], E. Beiser [ad], P. Berghaus [aw], D. Berley [q], E. Bernardini [aw], A. Bernhard [ag], D.Z. Besson [ab], G. Binder [h,g], D. Bindig [av], M. Bissok [a], E. Blaufuss [q], J. Blumenthal [a], D.J. Boersma [au], C. Bohm [an], M. Börner [u], F. Bos [j], D. Bose [ap], S. Böser [ae,*], O. Botner [au], J. Braun [ad], L. Brayeur [m], H.-P. Bretz [aw], N. Buzinsky [w], J. Casey [e], M. Casier [m], E. Cheung [q], D. Chirkin [ad], A. Christov [y], K. Clark [aq,*], L. Classen [x], S. Coenders [ag], G.H. Collin [n], J.M. Conrad [n], D.F. Cowen [at,as], A.H. Cruz Silva [aw], J. Daughhetee [e], J.C. Davis [r], M. Day [ad], J.P.A.M. de André [v], C. De Clercq [m], E. del Pino Rosendo [ae], H. Dembinski [ah], S. De Ridder [z], P. Desiati [ad], K.D. de Vries [m], G. de Wasseige [m], M. de With [i], T. DeYoung [v], J.C. Díaz-Vélez [ad], V. di Lorenzo [ae], J.P. Dumm [an], M. Dunkman [at], B. Eberhardt [ae], T. Ehrhardt [ae], B. Eichmann [j], S. Euler [au], P.A. Evenson [ah], S. Fahey [ad], A.R. Fazely [f], J. Feintzeig [ad], J. Felde [q], K. Filimonov [g], C. Finley [an], S. Flis [an], C.-C. Fösig [ae], T. Fuchs [u], T.K. Gaisser [ah], R. Gaior [o], J. Gallagher [ac], L. Gerhardt [h,g], K. Ghorbani [ad], D. Gier [a], L. Gladstone [ad], M. Glagla [a], T. Glüsenkamp [aw], A. Goldschmidt [h], G. Golup [m], J.G. Gonzalez [ah], D. Góra [aw], D. Grant [w,*], Z. Griffith [ad], A. Groß [ag], C. Ha [h,g], C. Haack [a], A. Haj Ismail [z], A. Hallgren [au], F. Halzen [ad], E. Hansen [t], B. Hansmann [a], K. Hanson [ad], D. Hebecker [i], D. Heereman [l], K. Helbing [av], R. Hellauer [q], S. Hickford [av], J. Hignight [v], G.C. Hill [b], K.D. Hoffman [q], R. Hoffmann [av], K. Holzapfel [ag], A. Homeier [k], K. Hoshina [ad,1], F. Huang [at], M. Huber [ag], W. Huelsnitz [q], P.O. Hulth [an],

http://dx.doi.org/10.1016/j.nuclphysb.2016.03.028

K. Hultqvist [an], S. In [ap], A. Ishihara [o], E. Jacobi [aw], G.S. Japaridze [d], M. Jeong [ap], K. Jero [ad], B.J.P. Jones [n], M. Jurkovic [ag], A. Kappes [x], T. Karg [aw], A. Karle [ad], M. Kauer [ad,ai], A. Keivani [at], J.L. Kelley [ad], J. Kemp [a], A. Kheirandish [ad], J. Kiryluk [ao], S.R. Klein [h,g], G. Kohnen [af], R. Koirala [ah], H. Kolanoski [i], R. Konietz [a], L. Köpke [ae], C. Kopper [w], S. Kopper [av], D.J. Koskinen [t,*], M. Kowalski [i,aw], K. Krings [ag], G. Kroll [ae], M. Kroll [j], G. Krückl [ae], J. Kunnen [m], N. Kurahashi [ak], T. Kuwabara [o], M. Labare [z], J.L. Lanfranchi [at], M.J. Larson [t], M. Lesiak-Bzdak [ao], M. Leuermann [a], J. Leuner [a], L. Lu [o], J. Lünemann [m], J. Madsen [am], G. Maggi [m], K.B.M. Mahn [v], M. Mandelartz [j], R. Maruyama [ai], K. Mase [o], H.S. Matis [h], R. Maunu [q], F. McNally [ad], K. Meagher [l], M. Medici [t], A. Meli [z], T. Menne [u], G. Merino [ad], T. Meures [l], S. Miarecki [h,g], E. Middell [aw], L. Mohrmann [aw], T. Montaruli [y], R. Morse [ad], R. Nahnhauer [aw], U. Naumann [av], G. Neer [v], H. Niederhausen [ao], S.C. Nowicki [w], D.R. Nygren [h], A. Obertacke Pollmann [av], A. Olivas [q], A. Omairat [av], A. O'Murchadha [l], T. Palczewski [ar], H. Pandya [ah], D.V. Pankova [at], L. Paul [a], J.A. Pepper [ar], C. Pérez de los Heros [au], C. Pfendner [r], D. Pieloth [u], E. Pinat [l], J. Posselt [av], P.B. Price [g], G.T. Przybylski [h], M. Quinnan [at], C. Raab [l], L. Rädel [a], M. Rameez [y], K. Rawlins [c], R. Reimann [a], M. Relich [o], E. Resconi [ag], W. Rhode [u], M. Richman [ak], S. Richter [ad], B. Riedel [w], S. Robertson [b], M. Rongen [a], C. Rott [ap], T. Ruhe [u], D. Ryckbosch [z], L. Sabbatini [ad], H.-G. Sander [ae], A. Sandrock [u], J. Sandroos [ae], S. Sarkar [t,aj], K. Schatto [ae], M. Schimp [a], T. Schmidt [q], S. Schoenen [a], S. Schöneberg [j], A. Schönwald [aw], L. Schulte [k], L. Schumacher [a], D. Seckel [ah], S. Seunarine [am], D. Soldin [av], M. Song [q], G.M. Spiczak [am], C. Spiering [aw], M. Stahlberg [a], M. Stamatikos [r,2], T. Stanev [ah], A. Stasik [aw], A. Steuer [ae], T. Stezelberger [h], R.G. Stokstad [h], A. Stößl [aw], R. Ström [au], N.L. Strotjohann [aw], G.W. Sullivan [q], M. Sutherland [r], H. Taavola [au], I. Taboada [e], J. Tatar [h,g], S. Ter-Antonyan [f], A. Terliuk [aw], G. Tešić [at], S. Tilav [ah], P.A. Toale [ar], M.N. Tobin [ad], S. Toscano [m], D. Tosi [ad], M. Tselengidou [x], A. Turcati [ag], E. Unger [au], M. Usner [aw], S. Vallecorsa [y], J. Vandenbroucke [ad], N. van Eijndhoven [m], S. Vanheule [z], J. van Santen [aw], J. Veenkamp [ag], M. Vehring [a], M. Voge [k], M. Vraeghe [z], C. Walck [an], A. Wallace [b], M. Wallraff [a], N. Wandkowsky [ad], Ch. Weaver [w], C. Wendt [ad], S. Westerhoff [ad], B.J. Whelan [b], K. Wiebe [ae], C.H. Wiebusch [a], L. Wille [ad], D.R. Williams [ar], L. Wills [ak], H. Wissing [q], M. Wolf [an], T.R. Wood [w],

K. Woschnagg [g], D.L. Xu [ad], X.W. Xu [f], Y. Xu [ao], J.P. Yanez [aw], G. Yodh [aa], S. Yoshida [o], M. Zoll [an]

[a] *III. Physikalisches Institut, RWTH Aachen University, D-52056 Aachen, Germany*
[b] *Department of Physics, University of Adelaide, Adelaide, 5005, Australia*
[c] *Dept. of Physics and Astronomy, University of Alaska Anchorage, 3211 Providence Dr., Anchorage, AK 99508, USA*
[d] *CTSPS, Clark-Atlanta University, Atlanta, GA 30314, USA*
[e] *School of Physics and Center for Relativistic Astrophysics, Georgia Institute of Technology, Atlanta, GA 30332, USA*
[f] *Dept. of Physics, Southern University, Baton Rouge, LA 70813, USA*
[g] *Dept. of Physics, University of California, Berkeley, CA 94720, USA*
[h] *Lawrence Berkeley National Laboratory, Berkeley, CA 94720, USA*
[i] *Institut für Physik, Humboldt-Universität zu Berlin, D-12489 Berlin, Germany*
[j] *Fakultät für Physik & Astronomie, Ruhr-Universität Bochum, D-44780 Bochum, Germany*
[k] *Physikalisches Institut, Universität Bonn, Nussallee 12, D-53115 Bonn, Germany*
[l] *Université Libre de Bruxelles, Science Faculty CP230, B-1050 Brussels, Belgium*
[m] *Vrije Universiteit Brussel, Dienst ELEM, B-1050 Brussels, Belgium*
[n] *Dept. of Physics, Massachusetts Institute of Technology, Cambridge, MA 02139, USA*
[o] *Dept. of Physics, Chiba University, Chiba 263-8522, Japan*
[p] *Dept. of Physics and Astronomy, University of Canterbury, Private Bag 4800, Christchurch, New Zealand*
[q] *Dept. of Physics, University of Maryland, College Park, MD 20742, USA*
[r] *Dept. of Physics and Center for Cosmology and Astro-Particle Physics, Ohio State University, Columbus, OH 43210, USA*
[s] *Dept. of Astronomy, Ohio State University, Columbus, OH 43210, USA*
[t] *Niels Bohr Institute, University of Copenhagen, DK-2100 Copenhagen, Denmark*
[u] *Dept. of Physics, TU Dortmund University, D-44221 Dortmund, Germany*
[v] *Dept. of Physics and Astronomy, Michigan State University, East Lansing, MI 48824, USA*
[w] *Dept. of Physics, University of Alberta, Edmonton, Alberta, T6G 2E1, Canada*
[x] *Erlangen Centre for Astroparticle Physics, Friedrich-Alexander-Universität Erlangen-Nürnberg, D-91058 Erlangen, Germany*
[y] *Département de physique nucléaire et corpusculaire, Université de Genève, CH-1211 Genève, Switzerland*
[z] *Dept. of Physics and Astronomy, University of Gent, B-9000 Gent, Belgium*
[aa] *Dept. of Physics and Astronomy, University of California, Irvine, CA 92697, USA*
[ab] *Dept. of Physics and Astronomy, University of Kansas, Lawrence, KS 66045, USA*
[ac] *Dept. of Astronomy, University of Wisconsin, Madison, WI 53706, USA*
[ad] *Dept. of Physics and Wisconsin IceCube Particle Astrophysics Center, University of Wisconsin, Madison, WI 53706, USA*
[ae] *Institute of Physics, University of Mainz, Staudinger Weg 7, D-55099 Mainz, Germany*
[af] *Université de Mons, 7000 Mons, Belgium*
[ag] *Technische Universität München, D-85748 Garching, Germany*
[ah] *Bartol Research Institute and Dept. of Physics and Astronomy, University of Delaware, Newark, DE 19716, USA*
[ai] *Dept. of Physics, Yale University, New Haven, CT 06520, USA*
[aj] *Dept. of Physics, University of Oxford, 1 Keble Road, Oxford OX1 3NP, UK*
[ak] *Dept. of Physics, Drexel University, 3141 Chestnut Street, Philadelphia, PA 19104, USA*
[al] *Physics Department, South Dakota School of Mines and Technology, Rapid City, SD 57701, USA*
[am] *Dept. of Physics, University of Wisconsin, River Falls, WI 54022, USA*
[an] *Oskar Klein Centre and Dept. of Physics, Stockholm University, SE-10691 Stockholm, Sweden*
[ao] *Dept. of Physics and Astronomy, Stony Brook University, Stony Brook, NY 11794-3800, USA*
[ap] *Dept. of Physics, Sungkyunkwan University, Suwon 440-746, Republic of Korea*
[aq] *Dept. of Physics, University of Toronto, Toronto, Ontario, M5S 1A7, Canada*
[ar] *Dept. of Physics and Astronomy, University of Alabama, Tuscaloosa, AL 35487, USA*
[as] *Dept. of Astronomy and Astrophysics, Pennsylvania State University, University Park, PA 16802, USA*
[at] *Dept. of Physics, Pennsylvania State University, University Park, PA 16802, USA*
[au] *Dept. of Physics and Astronomy, Uppsala University, Box 516, S-75120 Uppsala, Sweden*
[av] *Dept. of Physics, University of Wuppertal, D-42119 Wuppertal, Germany*
[aw] *DESY, D-15735 Zeuthen, Germany*

Received 31 January 2016; received in revised form 9 March 2016; accepted 23 March 2016
Available online 30 March 2016
Editor: Tommy Ohlsson

Abstract

IceCube, a gigaton-scale neutrino detector located at the South Pole, was primarily designed to search for astrophysical neutrinos with energies of PeV and higher. This goal has been achieved with the detection of the highest energy neutrinos to date. At the other end of the energy spectrum, the DeepCore extension lowers the energy threshold of the detector to approximately 10 GeV and opens the door for oscillation studies using atmospheric neutrinos. An analysis of the disappearance of these neutrinos has been completed, with the results produced being complementary with dedicated oscillation experiments. Following a review of the detector principle and performance, the method used to make these calculations, as well as the results, is detailed. Finally, the future prospects of IceCube-DeepCore and the next generation of neutrino experiments at the South Pole (IceCube-Gen2, specifically the PINGU sub-detector) are briefly discussed.

1. Introduction

It is currently well known that neutrinos oscillate [1] and, in fact, the writing of this document celebrates the acknowledgement of the effort of pioneers in the field of neutrino oscillation. This field has been the subject of intensive study for decades, with recent results indicating that the time of precision studies of the oscillation mechanism has arrived. Many experiments have contributed to our understanding of the neutrino oscillation mechanism, with several currently in operation and many more planned for the future [2]. One of the more recent contributors to the understanding of the neutrino oscillation framework is the IceCube detector [3], specifically through the use of the DeepCore extension [4], which will be discussed here.

Due to the nature of this publication, the mechanics of neutrino oscillation will not be reviewed here. Instead we discuss the oscillation analyses that primarily concern the propagation of muon-type neutrinos, although the use of electron-type neutrinos may also become important in future detectors. The most relevant quantity is the probability that a neutrino produced as a muon-type is detected as the same type following propagation. This probability can be expressed for vacuum oscillations, as shown in Equation (1), in which L[km] represents the distance travelled and E[GeV] represents the neutrino energy.

$$P_{\nu_\mu \to \nu_\mu} \approx 1 - \sin^2 2\theta_{23} \sin^2 \left[1.27 \Delta m^2_{32} L/E \right] \tag{1}$$

In Equation (1), the mixing angle (θ_{23}) as well as the mass difference (Δm^2_{32}) between the second and third mass eigenstates are the only oscillation parameters included. This is a good

* Corresponding authors.
E-mail addresses: sboeser@uni-mainz.de (S. Böser), kclark@physics.utoronto.ca (K. Clark), drg@ualberta.ca (D. Grant), koskinen@nbi.ku.dk (D.J. Koskinen).
[1] Earthquake Research Institute, University of Tokyo, Bunkyo, Tokyo 113-0032, Japan.
[2] NASA Goddard Space Flight Center, Greenbelt, MD 20771, USA.

approximation at neutrino energies above roughly 15 GeV and assuming three neutrino flavours. At lower energies, mixing with the first neutrino mass eigenstate must be considered, requiring Equation (1) to be extended. In addition to the inclusion of the first mass eigenstate, further modifications of the oscillation probability must be applied to account for the effect of matter on the propagation. This effect was first described by Wolfenstein, Mikheyev, and Smirnov and is called the MSW effect [5,6]. Examining propagation of neutrinos through the Earth and assuming the PREM density profile [7], this modulation has its largest impact at a neutrino energy of 6.2 GeV and a cosine of the zenith angle of -0.68. Even with these corrections, the L/E dependence of Equation (1) on the phase of the oscillation probability remains unchanged. This is the focus of the current DeepCore measurements.

Examination of the survival probability for muon-type neutrinos has shown that there is also a parametric resonance that must be considered. The resonance has been well described [8], and shows a large effect for neutrino energies less than 7 GeV and with the cosine of the zenith angle (the metric used to define the path length through the Earth of the incoming neutrino) less than -0.68. At these angles, the low-energy oscillations are enhanced because of the "step" in the Earth's density at the core. While the impact of the parametric resonance and MSW effect is minimal in the DeepCore analyses discussed next, it must be taken into consideration for the planned future atmospheric measurements detailed at the conclusion of this note.

2. Detector

The IceCube detector [9] is a three-dimensional array of photosensors deployed in the deep glacial ice at the South Pole, designed to detect the light produced in neutrino interactions. Neutrinos interact in one of two ways in the ice; a neutral current interaction which exchanges a Z^0 and produces a shower of hadrons and a charged-current interaction which exchanges a $W^{\pm}$ and produces a charged lepton. As the secondary particles travel faster than the speed of light in the medium, Cherenkov radiation is generated, which is detected by the detector.

Events in the IceCube detector are separable using the interaction type. When a muon-type neutrino undergoes a charged current interaction, a muon is produced that will generate light along its path which, depending on the energy, could extend for kilometres. The signature of this event in the detector gives rise to the classification in IceCube as "track-like".

For all neutral-current interactions, a "shower" of hadrons is produced at the interaction vertex, accompanying the outgoing neutrino. This classification of event is referred to as "cascade-like" because of the localized production of hadrons. This same shape is produced by the charged-current interaction of electron-type neutrinos where the outgoing particle causes an electromagnetic shower. Finally, tau-type neutrinos can undergo a charged-current interaction whereby the tau lepton decays to a muon, producing a track-like signature or, for the majority of cases, an electromagnetic shower and cascade-like signature. Due to the low cross-section and branching ratio, this event type is significantly suppressed at energies relevant to the atmospheric oscillation analysis discussed here.

The IceCube photosensors that detect the neutrino interaction light are deployed on long "strings" which extend more than two and a half kilometres in the ice. The instrumentation on each of the strings begins 1450 m below the ice surface and extends vertically for roughly one kilometre. Each string has 60 PMTs situated in glass spheres along with the associated electronics [3] to make up a Digital Optical Module (or DOM). The IceCube detector has 78 strings which are separated by roughly 125 m and the DOMs on the strings themselves are separated vertically by 17 m (see Fig. 1). This configuration instruments roughly a gigaton of the ice, a

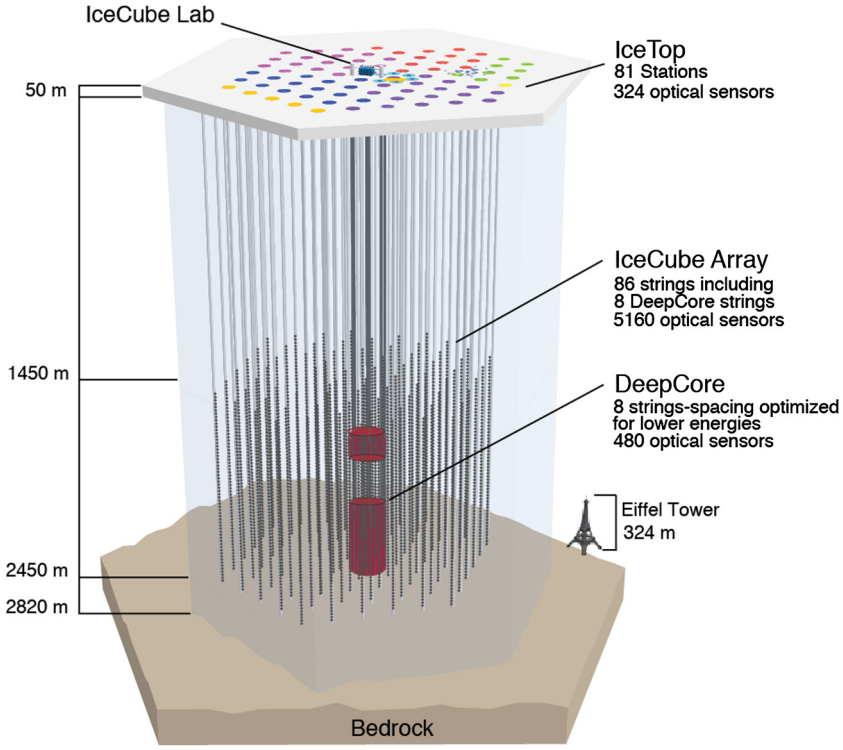

Fig. 1. Artist cross-section of the IceCube detector, showing the IceTop array at the surface of the ice and the IceCube array roughly 1.5 km below. The DeepCore strings are shown in the shaded region at the middle of the IceCube detector. (For interpretation of the colours in this figure, the reader is referred to the web version of this article.)

volume of one cubic kilometre, with 4680 ten inch photomultiplier tubes (PMTs) [10] laid out in a roughly hexagonal grid as shown in Fig. 1, which includes the IceTop array [11].

The primary goal of the IceCube detector is to study high-energy neutrinos produced in astrophysical sources, which have a very low flux and therefore require a large target mass. IceCube reported the discovery of a high-energy neutrino flux [12] utilizing an analysis that demanded each event start inside the instrumented fiducial mass and deposit more than 30 TeV in energy. The flavour ratio of the high-energy neutrinos (between 25 TeV and 2.8 PeV) has been measured [13], and provides constraints on both astrophysical production mechanisms and fundamental physics. The sensitivity of the high energy neutrino flavour ratio to neutrino oscillations was recognized even before IceCube was built [13], and the possibility to search for new physics through the oscillations of high energy neutrinos has been examined by several authors [14–17].

It was also recognized [18–21,8] that a slightly lower energy threshold would provide a copious flux of atmospheric neutrinos in the range of L/E (see Eq. (1)) relevant to neutrino flavour oscillations, opening a window of opportunity to study neutrino physics in the ice. A reduced energy threshold provides several other advantages, including enhanced sensitivity to dark matter, specifically through searching for WIMP annihilations in the Sun, the Galactic Centre, and the Halo. The searches for galactic supernova neutrinos, slow moving monopoles, and low energy neutrinos from astrophysical sources add to the motivation for this extension.

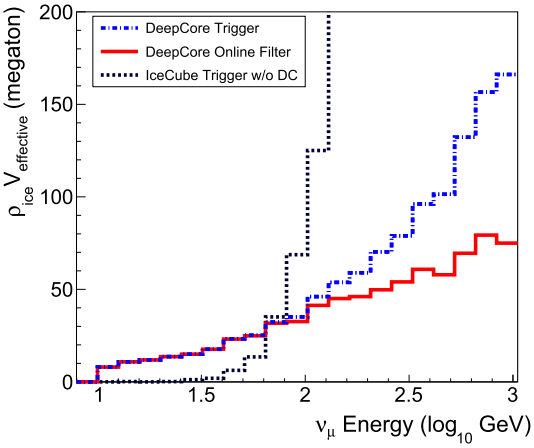

Fig. 2. The effective mass (effective volume times density) of the IceCube and DeepCore detectors, showing the effect of the additional strings. Shown here is the effective mass for ν_μ.

2.1. DeepCore

In order to lower the neutrino-energy detection threshold, eight strings were installed in the centre of the IceCube detector, which are separate from the hexagonal grid, referred to as the DeepCore extension. The string-to-string spacing for these additional sensors is between 40 and 70 m and the DOMs are located on the strings with a reduced spacing of 7 m for the lowest 50 DOMs. The location of the strings can be seen in Fig. 1, in which the DeepCore strings are shown in the red cylinder.

The design of the DeepCore strings was aided considerably by the information obtained from operation of the AMANDA detector [22] (the predecessor to IceCube). As seen in Fig. 1, the DeepCore DOMs are deployed to avoid a portion of the ice found to have a dust concentration that was much higher than the surrounding ice [23], and demonstrated by the IceCube Collaboration to have a distinct increase in the light absorption. The DOM-to-DOM spacing for the photodetectors located above this "dust layer" is 10 m instead of the 7 m used on the rest of the string to provide an atmospheric-muon veto cap above the primary DeepCore array.

In addition to the photodetector density changes, roughly 75% of the PMTs on DeepCore strings have a higher quantum efficiency (approximately 1.39 times the efficiency of the standard IceCube DOMs [4]). These changes (the increase in the density of photodetectors in the ice and the increase in the efficiency of the PMTs) lowered the energy threshold for neutrino detection as shown in Fig. 2 for muon-type neutrinos.

It is clear from Fig. 2 that these eight strings have a significant impact on the sensitivity of the detector to low-energy (10 GeV $\leq E \leq$ 100 GeV) neutrinos, precisely the range of interest considered for studies of atmospheric neutrino oscillation. In addition to the lowered energy threshold, the DeepCore detector extension benefits from being located at the centre of the IceCube detector. The IceCube DOMs surrounding the DeepCore strings provide an excellent veto against incoming muons that could otherwise be mistaken for neutrinos produced in the atmosphere [4].

In addition to the hardware differences described above, updates to the trigger were also necessitated by the lower-energy events to produce the gains shown in Fig. 2. The required number

of coincident pairs of hits was lowered from eight to three, producing a new trigger more sensitive to low-light events. Applying these hardware and software changes, the detection threshold of the DeepCore extension is lowered and the noise background is reduced so that the signal from neutrinos generated in the atmosphere is more easily identified.

3. Atmospheric neutrinos

The atmosphere of the Earth is constantly being bombarded by cosmic rays, primarily made up of protons and helium nuclei produced by astrophysical objects [1]. These cosmic rays have been observed over a wide range of energy, from 10^9 to 10^{20} eV.

The incoming cosmic rays interact with nucleons in the atmosphere surrounding the Earth causing hadronic cascades that, in turn, produce mesons, primarily pions and kaons. The first interactions occur roughly 20 km above the Earth, although heavier nuclei (of which there are few) can interact at higher altitudes. The resulting cascade includes an electromagnetic portion, occurring primarily through the decay of the π^0 to two photons that subsequently create additional photons and electrons.

In the hadronic portion of the cascade, pions are copiously produced and make up more than 99% of the particles [1]. The decays of these pions produce neutrinos as well as muons that can go on to decay into electrons and more neutrinos. An example (for the π^+) is shown in Equation (2). An analogous equation exists for the interaction involving the π^-.

$$\begin{aligned} p^+ + N &\rightarrow \pi^+ + \mathit{hadrons} \\ &\hookrightarrow \mu^+ + \nu_\mu \\ &\quad \hookrightarrow e^+ + \nu_e + \bar{\nu}_\mu \end{aligned} \tag{2}$$

The process shown in Equation (2) holds for muons having energies less than a few GeV that decay in the atmosphere. Muons with higher energies have a high probability of reaching the Earth before decaying, and are the primary source of background for neutrino studies, discussed next.

3.1. Background

The dominant source of background for this analysis are atmospheric muons produced in cosmic ray showers, e.g. the second line in Equation (2). For each atmospheric neutrino interaction detected, roughly 10^6 muons trigger the detector [4]. A large portion of this flux is relatively simple to remove given DeepCore's location at the centre of IceCube. In order to exploit the advantage of having the DOMs surrounding the DeepCore detector, a specific cut (filter) was created for the low-energy data. This filter runs over triggered events and determines if there are hits in the "veto region" that are causally connected (based on the speed of light in the ice) to the hits recorded in DeepCore. The removal of these events provides a more pure sample on which to run the analysis.

4. Analysis

In order to study the neutrino oscillation parameters, there are two particularly important actions taken on the data: the event selection and the reconstruction. Once these are defined so that the background events are largely removed and the parameters of the original neutrino are

known, the more precise version of Equation (1) [1] can be used to extract the values of the mixing angle and the difference between the squared masses. Each of these vital aspects of the analysis will be addressed separately.

4.1. Event selection

The primary goal of the event selection is to ensure that the final data set is composed mostly of track-like events. There are still a significant number of atmospheric muons left in the data sample. These primarily consist of muons that have passed between the IceCube strings, avoiding detection, and therefore not being removed by the IceCube veto. The applied cut examines the position of the earliest DOM involved in the trigger, requiring it to be within the DeepCore fiducial volume. The total charge due to photons in the DOMs before the trigger (and that above the fiducial volume), as well as the charge collected as a function of time, are also used to remove these background events. The most significant cut is the use of the number of DOMs that record a hit (their signal is above the signal threshold) in coincidence with the photons expected from an atmospheric muon. In order to perform this cut, a muon hypothesis is generated and the likelihood of the event fitting with that hypothesis is calculated. If the likelihood is above the set threshold, the event is removed.

The final cut is to only analyze events that have a zenith angle such that they are entering the detector from below the horizon. This serves to dramatically reduce the number of atmospheric muons while retaining a sufficient amount of neutrinos to perform an analysis, roughly 40% [24].

In addition to filtering events not caused by neutrino interactions, it is also advantageous to remove events that, while they may be due to neutrinos, are not of sufficient quality for use in the final analysis and would reconstruct poorly (if at all). These events can be identified by looking at the "direct photons" that are detected (those that have undergone minimal scattering as they travel through the ice, which would delay the arrival of the photon at the PMT). The lack of scattering means that these photons are preferable for use in reconstructions.

The analyses discussed here apply a specific method to remove scattered photons. In this case, the "primary" DOM is identified where the most charge is collected, defining a starting point for the cut calculation. Using the time of the hit at this DOM, other photons can be identified with respect to their scattering by determining the time light takes to travel between the DOMs including an acceptable delay time. In this case, the delay time was set to 20 ns to allow for some minimal scattering in the ice. In addition to the timing information, it is expected that the pattern of hits from direct photons will produce a hyperbolic shape on the string as a function of time and position (see Fig. 3b) [24].

From the description above, the subsequent application of the event selection cuts provides the final sample. Fig. 4 illustrates the cumulative effects of the cut application, where the first cut (the use of the veto strings) significantly reduces the flux of mis-reconstructed atmospheric muons in the zenith range of interest (defined as up-going, or $-1.0 < \cos(\theta_{reco}) < 0.0$) while having very little effect on the simulated neutrino signal. The effect of the second cut (shown in the third panel) adds the remainder of the cuts previously described. The effect on the neutrino simulation is still very small while the up-going atmospheric muons are largely removed. The excess of atmospheric muons at an angle of $\cos(\theta_{reco}) \approx 0.3$ is the result of muons that are not tagged by the veto cut, but these are not used in the final analysis since they are identified as down-going.

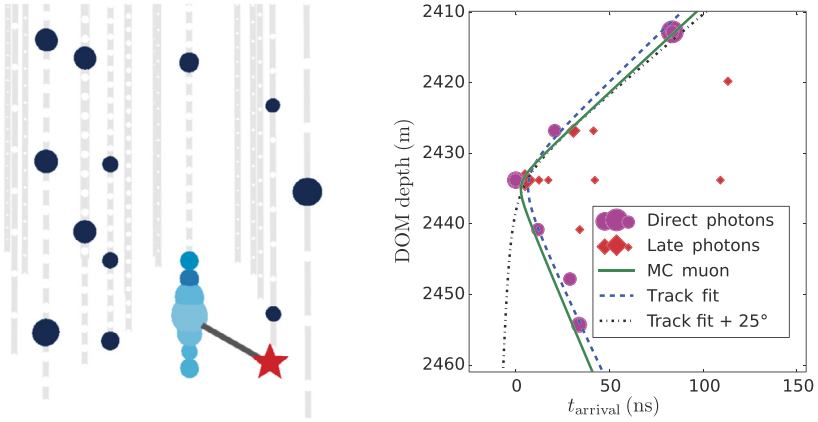

(a) Event side view.

(b) Time and position projection onto one string.

Fig. 3. A simulated 12 GeV ν_μ interacting in DeepCore and producing an 8 GeV muon (42 m range) and a 4 GeV hadronic shower. In (a), the event is shown with the interaction vertex marked with the red star, the strings shown in dashed lines and the hits indicated with spheres, where their size is proportional to the observed charge. The depth vs arrival time expectation using direct photons is shown in (b), with the hyperbolic shape explicit and the late photons shown in red squares. The expected hyperbolae from simulation, a track fit and the same fit altered by 25° are also shown. (For interpretation of the references to colour in this figure legend, the reader is referred to the web version of this article.)

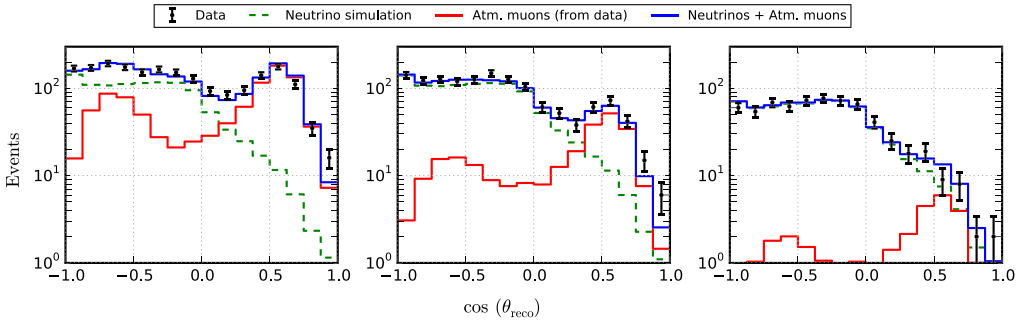

Fig. 4. Zenith angle distribution of data (black points), neutrino simulation (green dashed line), atmospheric muons (red line), and the combination of atmospheric muons and neutrinos (blue line) showing the effect of the event selection cuts. The first plot shows the total event distributions while the second plot uses the IceCube veto strings to remove atmospheric muons. The third plot adds a cut on the charge collected before the trigger. Taken from [24]. (For interpretation of the references to colour in this figure legend, the reader is referred to the web version of this article.)

4.2. Reconstruction

Once events are selected for inclusion in the analysis using these cuts, the timing information of the arrival at the DOM is used to fit one of two hypotheses for the emission of light; generation by a cascade-like or a track-like event. The light generated from these two hypotheses creates a different pattern of hits on the DOMs so that they can be distinguished. Both of these hypotheses can be fit using likelihood calculation algorithms and the most likely choice will be used. As discussed previously, one of the strengths of this analysis is the use of only muon-type neutrinos

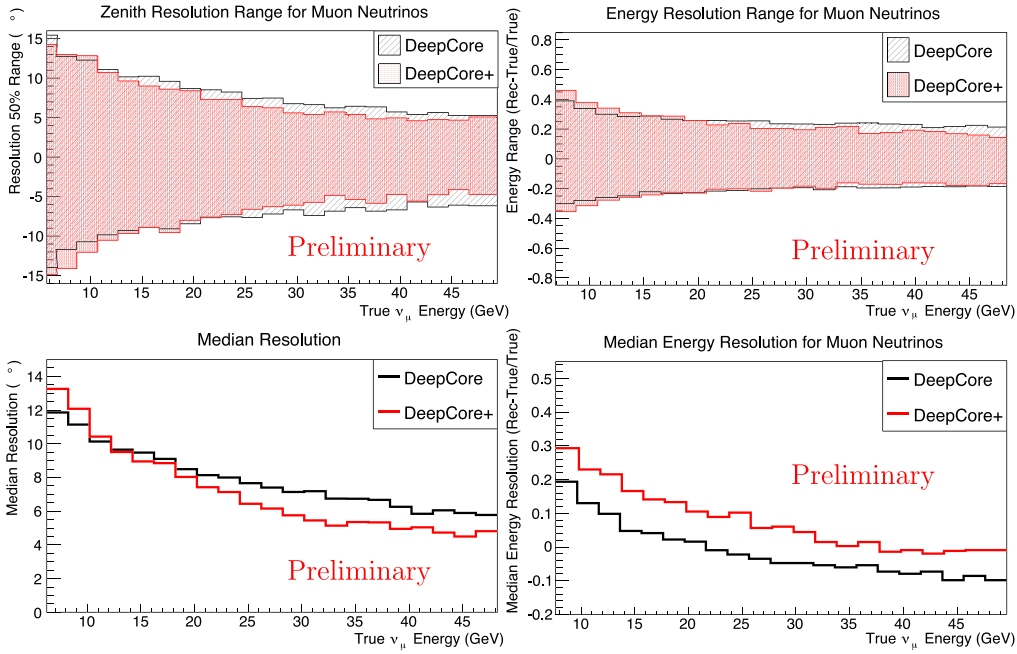

(a) Zenith resolution. (b) Energy resolution.

Fig. 5. Zenith and Energy resolution for both the published DeepCore analysis (labelled DeepCore) and the "improved" DeepCore analysis (labelled DeepCore+ and discussed in Section 6.1). (For interpretation of the references to colour in this figure legend, the reader is referred to the web version of this article.)

that have undergone a charged current interaction and therefore produced a muon. The benefit of using these events is that they are easily separable from all other types of interactions and the sample can be extracted with higher purity.

In the oscillation analysis, the zenith angle stands in for the L portion of the L/E ratio, required for the study. In order to use this ratio, the energy of the incoming neutrino must also be reconstructed from the data collected by the PMTs. The energy of the selected events is determined using the interactions of the muon-type neutrinos, modelled as a hadronic shower at the interaction vertex, as well as a track produced by the muon. The brightness of the hadronic shower at the interaction vertex is directly proportional to the energy of the hadrons, while the length of the track provides the energy of the muon. The sum of these two components provides an estimation of the total energy of the neutrino. The results of the reconstruction of both the zenith angle and the energy are shown in Fig. 5.

4.3. Systematics

The effects of systematic uncertainties in this analysis are also crucial to consider. These have been included as nuisance parameters in the fitting procedure, which holds the oscillation parameters not directly involved in the fit fixed. The systematics are broadly separated into three categories according to the way in which the effects' systematic variations are managed.

The first category of systematics are those that have an effect on the number of neutrinos (and anti-neutrinos) in the sample. This category includes:

- the level of contamination from atmospheric muons that trigger the detector,
- the atmospheric neutrino flux,
- the ratio of ν_e to ν_μ production, and
- the index of the neutrino energy spectrum.

A second class of systematic uncertainties deals with the propagation and collection of the light produced in the events. These systematics are:

- the photon collection efficiency of the DOMs,
- the scattering of photons from the ice immediately surrounding the DOMs, and
- the transmission of photons through the bulk ice.

The final uncertainty is somewhat different from the others of this category because of the discrete nature of the models. IceCube has a limited number of ice models that are used in the production and fitting of the data [25] so that this uncertainty can be marginalized.

The cuts and reconstruction described previously are then used to perform a muon disappearance analysis which calculates the oscillation parameters associated with the measured spectrum.

5. Results

An oscillation analysis has been performed using 953 days of data [24], with a total of 5174 track-like events observed. If there were no neutrino oscillations, 6830 muon-type neutrinos would have been expected in this time period. The calculation of the oscillation parameters involves the binning of the data in the logarithm of the reconstructed energy between 6 and 56 GeV and the cosine of the reconstructed zenith angle between -1 and 0 (restricting the analysis to upgoing events only). A binned maximum likelihood method is then applied with the parameters of interest being the mixing angle θ_{23} and the mass splitting Δm^2_{32}. In this analysis the oscillation probabilities are calculated using the three-flavour scheme with all parameters fixed to values from [26] except θ_{13} which is treated as a nuisance parameter.

If the normal neutrino mass ordering is assumed (the case shown in Fig. 6), the best fit oscillation parameters are $\sin^2\theta_{23} = 0.53^{+0.09}_{-0.12}$ and $\Delta m^2_{32} = 2.72^{+0.19}_{-0.20} \times 10^{-3}$ eV^2. The results show no preference for the mass ordering, with the preferred values assuming the inverted ordering being $\sin^2\theta_{23} = 0.51^{+0.09}_{-0.11}$ and $\Delta m^2_{32} = -2.72^{+0.18}_{-0.21} \times 10^{-3}$ eV^2. The contours produced by this analysis (shown in Fig. 6) complement those extracted from other experiments designed specifically to study neutrino oscillations.

The observed neutrinos may be plotted in the more intuitive L/E format, shown in Fig. 7. The spectrum of the events used in the analysis is shown with the associated uncertainties as well as the "no oscillation" spectrum expected given the number of events observed. It is clear that the observed neutrinos deviate from the no-oscillation spectrum. Further, for the L/E values where no oscillation is expected, the observed and expected distributions match well, indicating that the scaling of the expected distribution without oscillation matches the data.

The results obtained from the DeepCore analysis used neutrinos in the energy range from roughly 10 to 60 GeV, which is an energy region to which other experiments are either largely insensitive or have an L that puts them beyond the minimum of interest in the oscillation probability function. Examining the experiments shown in Fig. 6, this energy range complements those employed by other collaborations, where each of the projects shown use lower energy neutrinos (with a maximum around 10 GeV, approximately the lower threshold for DeepCore) to determine

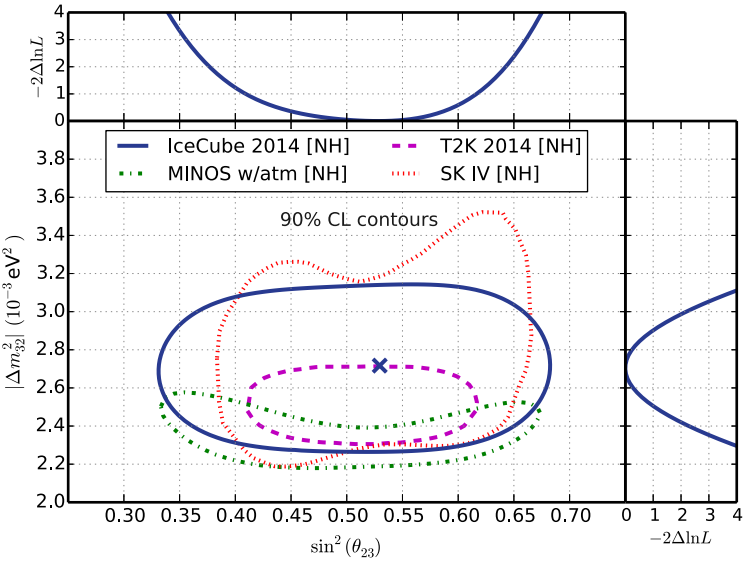

Fig. 6. The results of the DeepCore analysis showing the 90% contours of the current analysis along with that of MINOS [27], T2K [28], and SuperK [29].

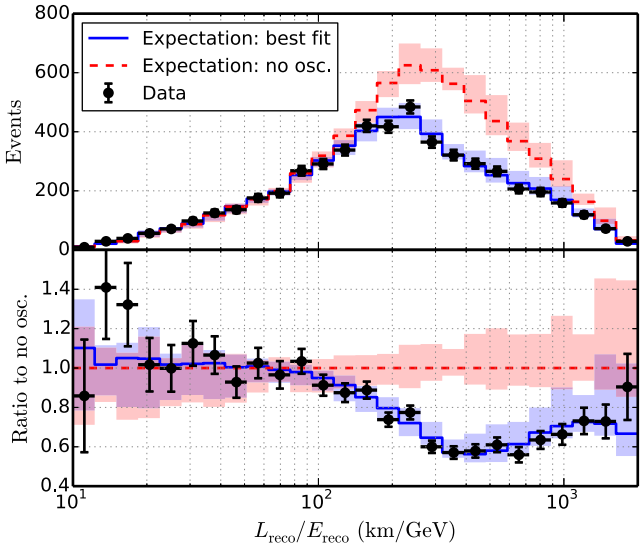

Fig. 7. The events from 953 days of data used in the analysis, plotted against L/E so that deviations arising from the oscillation can be seen. The solid line shows the best fit to the data while the dashed line illustrates the "no oscillation" scenario.

the parameters. It is an important test of neutrino physics over a wide range of energies that the results shown in Fig. 6, obtained using different energy ranges, are completely compatible.

6. Future

The DeepCore oscillation analysis has two main aspects that can be improved to provide an increased sensitivity to the parameters under study; the number of events in the data set (the "event selection") and the accuracy with which those events are reconstructed. There are, however, other oscillation-related topics of importance, namely the ordering of the neutrino masses, to which no anticipated improvements in DeepCore can provide sensitivity. As such, while work is on-going to improve DeepCore-related oscillation results, the deployment of additional photosensors in the deep ice is being planned to provide further improvements for current results and also probe a lower energy region with the necessary sensitivity for new oscillation physics. Here we briefly discuss these efforts.

6.1. Existing detector – DeepCore

In general, the changes aimed at improving the oscillation analysis focus on developing advanced techniques that can provide reliable reconstructions of the energy and zenith angle for a wider range of events than those selected in Section 5. Although Fig. 7 does not represent the method used to extract the oscillation parameters, it is clear that the uncertainty on the L/E parameter is a limitation of the process. Newly studied algorithms have shown that improvement on these reconstructions can be achieved.

In the improved reconstruction algorithm, the charge information from the DOM is binned in time and a likelihood is calculated using the arrival time of the photons at the DOMs. This method, while resource-intensive, has the advantage that all photons can be used instead of just those that are not scattered. Models of the scattering and absorption of the ice are used, as discussed with respect to the DeepCore systematics, to take these effects into account in the final likelihood. Using this method, significantly more events are included in the final data sample, and even events without muons of substantial track length can be reconstructed with improved precision. The impact of this change in algorithm is shown in Fig. 5.

As a consequence of being able to reliably reconstruct "lower quality" events, the neutrino selection efficiency is improved. Preliminary results from this updated analysis have shown that the increase in the number of events significantly improves the determination of the oscillation parameters. To continue to reduce the contours shown in Fig. 6 it will be necessary to alter the detector. DeepCore is still maturing, but no expected analysis improvements can open new oscillation topics, such as the neutrino mass ordering, except for a new detector configuration.

6.2. New detector – PINGU

Improvements in both the number of neutrino events in the sample and the precision of the event reconstruction can be enhanced simultaneously by increasing the density of photodetectors in the DeepCore volume. The examination of these changes has resulted in the planned detector known as the Precision IceCube Next Generation Upgrade (PINGU) [30].

The PINGU detector will be installed in the same location as DeepCore, at the centre of the IceCube strings, for similar experimental reasons. The veto capabilities of the IceCube detector are necessary to reduce the flux of atmospheric muons misidentified as neutrinos. The installation of the DeepCore detector has dramatically increased the knowledge of the optical transmission in the ice in this area, knowledge which has been applied to design of PINGU. The DOM-to-DOM distance (7 m with DeepCore) is lowered to 3 m in the preliminary PINGU design while the

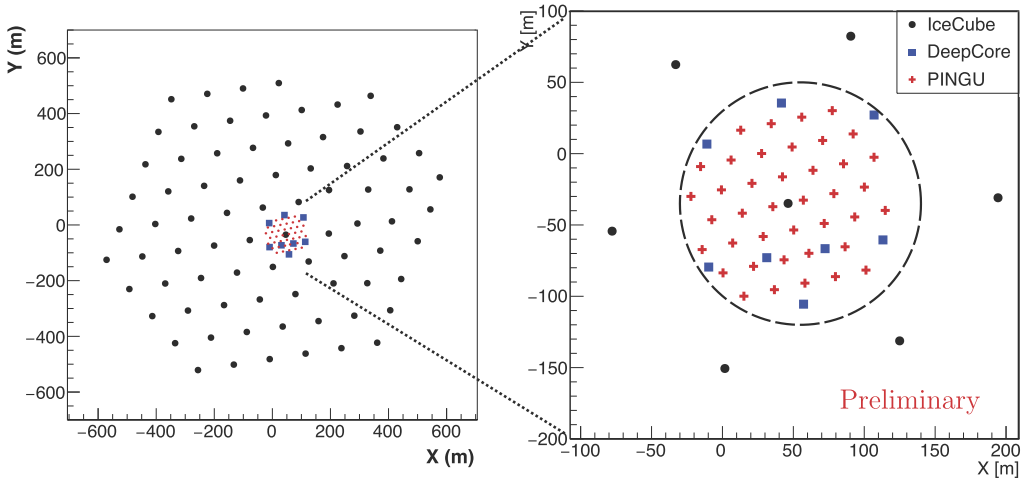

Fig. 8. Overhead view of IceCube, DeepCore, and PINGU. Note that while IceCube and DeepCore have 60 DOMs per string, PINGU has 96. Shown in the dashed line is the definition of the fiducial volume for the PINGU detector.

number of DOMs per string is increased from 50 (excluding the DOMs in the DeepCore top veto cap) to 96. A total of 40 new strings would be located within the DeepCore footprint, lowering the string-to-string spacing from between 40 and 70 m to 22 m, as shown in Fig. 8. The increase in photodetector density significantly improves the acceptance of low-energy (< 10 GeV) events compared to the DeepCore detector. Since the DeepCore strings are included in the PINGU detector, and the higher density does not increase the acceptance at high energy, the efficiency above 10 GeV remains largely the same while adding events down to roughly 1 GeV.

Given the detector design shown in Fig. 8, a suite of precision measurements becomes possible [30]. Using atmospheric neutrinos as the source, our knowledge of the neutrino oscillation parameters, shown in Fig. 6, may be dramatically improved to the point that PINGU would emerge as a leading project in the field. In a related search for tau-type neutrinos from oscillated atmospheric neutrinos, the preliminary studies indicate the ability to exclude ν_τ appearance after one month of data taking and a measurement on the predicted normalization to better than 10% after the first year. Equally intriguing is the potential for the detector to study the neutrino mass ordering. One of the fundamental remaining unknowns in the neutrino sector, the recently measured relatively large θ_{13} mixing angle makes it possible to utilize atmospheric neutrinos to definitely measure the mass ordering [8]. With the PINGU detector shown in Fig. 8, the design studies suggest the ability to identify the mass ordering with a precision of 3σ after approximately four years of data taking, depending on a normal or inverted ordering. Long term, a PINGU-scale detector has the potential to perform the first studies of the structure of the Earth's core using atmospheric neutrino tomography. Finally, the PINGU detector would have the ability to significantly improve the on-going IceCube-DeepCore research program, including world-leading indirect dark matter searches to lower particle masses, and sensitivity to supernova neutrinos.

7. Summary

The IceCube experiment has been the leading project in the search for high-energy neutrinos of astrophysical origin. With the inclusion of the DeepCore subarray, IceCube opened a window

to particle physics in the Antarctic, including measurement of the atmospheric neutrino oscillation parameters. There are improvements underway in the analysis of currently in-hand data that will further increase the precision on the oscillation parameter contours, cementing the position of DeepCore as a leading experiment in the field. Plans are also currently underway to further extend the reach of the IceCube facility into neutrino oscillation physics. The planned PINGU detector is expected to provide the ability not only to improve the constraints on the mixing parameters, but also answer several of the outstanding questions in neutrino physics today.

Acknowledgements

We acknowledge the support from the following agencies: U.S. National Science Foundation-Office of Polar Programs, U.S. National Science Foundation-Physics Division, University of Wisconsin Alumni Research Foundation, the Grid Laboratory Of Wisconsin (GLOW) grid infrastructure at the University of Wisconsin-Madison, the Open Science Grid (OSG) grid infrastructure; U.S. Department of Energy, and National Energy Research Scientific Computing Center, the Louisiana Optical Network Initiative (LONI) grid computing resources; Natural Sciences and Engineering Research Council of Canada, WestGrid and Compute/Calcul Canada; Swedish Research Council, Swedish Polar Research Secretariat, Swedish National Infrastructure for Computing (SNIC), and Knut and Alice Wallenberg Foundation, Sweden; German Ministry for Education and Research (BMBF), Deutsche Forschungsgemeinschaft (DFG), Helmholtz Alliance for Astroparticle Physics (HAP), Research Department of Plasmas with Complex Interactions (Bochum), Germany; Fund for Scientific Research (FNRS-FWO), FWO Odysseus programme, Flanders Institute to encourage scientific and technological research in industry (IWT), Belgian Federal Science Policy Office (Belspo); University Of Oxford, United Kingdom; Marsden Fund, New Zealand; Australian Research Council; Japan Society for Promotion of Science (JSPS); the Swiss National Science Foundation (SNSF), Switzerland; National Research Foundation of Korea (NRF); Villum Fonden, Danish National Research Foundation (DNRF), Denmark.

References

[1] K.A. Olive, et al., Review of particle physics, Chin. Phys. C 38 (2014) 090001.
[2] E. Kearns, G. Feldman (Eds.), Proceedings, 26th International Conference on Neutrino Physics and Astrophysics (Neutrino 2014), vol. 1666, 2015.
[3] R. Abbasi, et al., The IceCube data acquisition system: signal capture, digitization, and timestamping, Nucl. Instrum. Methods A 601 (2009) 294–316, arXiv:0810.4930.
[4] R. Abbasi, et al., The design and performance of IceCube DeepCore, Astropart. Phys. 35 (2012) 615–624, arXiv:1109.6096.
[5] L. Wolfenstein, Neutrino oscillations in matter, Phys. Rev. D 17 (1978) 2369–2374.
[6] S.P. Mikheev, A.Yu. Smirnov, Resonance amplification of oscillations in matter and spectroscopy of solar neutrinos, Sov. J. Nucl. Phys. 42 (1985) 913–917;
S.P. Mikheev, A.Yu. Smirnov, Yad. Fiz. 42 (1985) 1441.
[7] A.M. Dziewonski, D.L. Anderson, Preliminary reference earth model, Phys. Earth Planet. Inter. 25 (1981) 297–356.
[8] E.K. Akhmedov, S. Razzaque, A.Yu. Smirnov, Mass hierarchy, 2–3 mixing and CP-phase with huge atmospheric neutrino detectors, J. High Energy Phys. 02 (2013) 082, arXiv:1205.7071;
E.K. Akhmedov, S. Razzaque, A.Yu. Smirnov, J. High Energy Phys. 07 (2013) 026 (Erratum).
[9] F. Halzen, S.R. Klein, IceCube: an instrument for neutrino astronomy, Rev. Sci. Instrum. 81 (2010) 081101, http://dx.doi.org/10.1063/1.3480478, arXiv:1007.1247.
[10] R. Abbasi, et al., Calibration and characterization of the IceCube photomultiplier tube, Nucl. Instrum. Methods Phys. Res., Sect. A 618 (2010) 139–152, arXiv:1002.2442.

[11] R. Abbasi, et al., IceTop: the surface component of IceCube, The IceCube Collaboration, Nucl. Instrum. Methods Phys. Res., Sect. A 700 (2013) 188–220, arXiv:1207.6326.
[12] M.G. Aartsen, et al., Evidence for high-energy extraterrestrial neutrinos at the IceCube detector, Science 342 (2013) 1242856, arXiv:1311.5238.
[13] J.G. Learned, S. Pakvasa, Detecting tau-neutrino oscillations at PeV energies, Astropart. Phys. 3 (1995) 267–274, http://dx.doi.org/10.1016/0927-6505(94)00043-3, arXiv:hep-ph/9405296.
[14] J.F. Beacom, N.F. Bell, D. Hooper, S. Pakvasa, T.J. Weiler, Measuring flavor ratios of high-energy astrophysical neutrinos, Phys. Rev. D 68 (2003) 093005, http://dx.doi.org/10.1103/PhysRevD.68.093005, arXiv:hep-ph/0307025; J.F. Beacom, N.F. Bell, D. Hooper, S. Pakvasa, T.J. Weiler, Phys. Rev. D 72 (2005) 019901, http://dx.doi.org/10.1103/PhysRevD.72.019901 (Erratum).
[15] M.C. Gonzalez-Garcia, F. Halzen, M. Maltoni, Physics reach of high-energy and high-statistics icecube atmospheric neutrino data, Phys. Rev. D 71 (2005) 093010, http://dx.doi.org/10.1103/PhysRevD.71.093010, arXiv:hep-ph/0502223.
[16] M. Maltoni, W. Winter, Testing neutrino oscillations plus decay with neutrino telescopes, J. High Energy Phys. 07 (2008) 064, http://dx.doi.org/10.1088/1126-6708/2008/07/064, arXiv:0803.2050.
[17] L.A. Anchordoqui, et al., Cosmic neutrino pevatrons: a brand new pathway to astronomy, astrophysics, and particle physics, J. High Energy Astrophys. 1–2 (2014) 1–30, http://dx.doi.org/10.1016/j.jheap.2014.01.001, arXiv:1312.6587.
[18] I.F.M. Albuquerque, G.F. Smoot, Measuring atmospheric neutrino oscillations with neutrino telescopes, Phys. Rev. D 64 (2001) 053008, http://dx.doi.org/10.1103/PhysRevD.64.053008, arXiv:hep-ph/0102078.
[19] O. Mena, I. Mocioiu, S. Razzaque, Neutrino mass hierarchy extraction using atmospheric neutrinos in ice, Phys. Rev. D 78 (2008) 093003, http://dx.doi.org/10.1103/PhysRevD.78.093003, arXiv:0803.3044.
[20] G. Giordano, O. Mena, I. Mocioiu, Atmospheric neutrino oscillations and tau neutrinos in ice, Phys. Rev. D 81 (2010) 113008, http://dx.doi.org/10.1103/PhysRevD.81.113008, arXiv:1004.3519.
[21] S. Razzaque, A.Yu. Smirnov, Searching for sterile neutrinos in ice, J. High Energy Phys. 07 (2011) 084, http://dx.doi.org/10.1007/JHEP07(2011)084, arXiv:1104.1390.
[22] E. Andres, et al., Results from the AMANDA high-energy neutrino detector, Nucl. Phys. Proc. Suppl. 91 (2001) 423–430, arXiv:astro-ph/0009242.
[23] M. Ackermann, et al., Optical properties of deep glacial ice at the South Pole, J. Geophys. Res. 111 (D13) (2006) D13203.
[24] M. Aartsen, et al., Determining neutrino oscillation parameters from atmospheric muon neutrino disappearance with three years of IceCube DeepCore data, Phys. Rev. D 91 (7) (2015) 072004, arXiv:1410.7227.
[25] M. Aartsen, et al., Measurement of south pole ice transparency with the icecube LED calibration system, Nucl. Instrum. Methods Phys. Res., Sect. A, Accel. Spectrom. Detect. Assoc. Equip. 711 (2013) 73–89.
[26] G.L. Fogli, E. Lisi, A. Marrone, D. Montanino, A. Palazzo, A.M. Rotunno, Global analysis of neutrino masses, mixings, and phases: entering the era of leptonic CP violation searches, Phys. Rev. D 86 (2012) 013012.
[27] P. Adamson, et al., Measurement of neutrino and antineutrino oscillations using beam and atmospheric data in MINOS, Phys. Rev. Lett. 110 (25) (2013) 251801, arXiv:1304.6335.
[28] K. Abe, et al., Precise measurement of the neutrino mixing parameter θ_{23} from muon neutrino disappearance in an off-axis beam, Phys. Rev. Lett. 112 (18) (2014) 181801, arXiv:1403.1532.
[29] A. Himmel, Recent results from Super-Kamiokande, AIP Conf. Proc. 1604 (2014) 345–352, arXiv:1310.6677.
[30] M.G. Aartsen, et al., Letter of intent: The Precision IceCube Next Generation Upgrade (PINGU), arXiv:1401.2046.